JGS
Journal of the Geological Society

Research article

Published online July 19, 2019 https://doi.org/10.1144/jgs2019-031 | Vol. 176 | 2019 | pp. 1143–1153

Local to global controls on the deposition of organic-rich muds across the Late Jurassic Laurasian Seaway

Elizabeth Atar[1]*, Christian März[2], Bernhard Schnetger[3], Thomas Wagner[4] & Andrew Aplin[1]

[1] Department of Earth Sciences, Durham University, South Road, Durham, DH1 3LE, UK
[2] School of Earth and Environment, University of Leeds, Leeds, LS2 9JT, UK
[3] ICMB, Oldenburg University, P.O. Box 2503, 26111 Oldenburg, Germany
[4] Lyell Centre, Heriot-Watt University, Edinburgh, EH14 4AS, UK
EA, 0000-0003-1921-022X; CM, 0000-0003-2558-4711; AA, 0000-0001-8081-8723
*Correspondence: elizabeth.atar@gmail.com

Abstract: Muds deposited in large-scale epicontinental seaways provide deep insights into palaeoclimates, biogeochemical cycles, sedimentation processes and organic carbon burial during exceptionally warm periods throughout the Phanerozoic. Temporal changes can be monitored at single locations but the key, larger scale oceanographical and related biogeochemical processes are likely to be more clearly revealed by comparisons between individual sub-basins within seaways. Here, we compare inorganic geochemical records from the Jurassic (upper *Pectinatites wheatleyensis* to lower *Pectinatites pectinatus* ammonite zones) of the Swanworth Quarry 1 Core from the Wessex Basin (Dorset, UK) to time-equivalent records from the Ebberston 87 Core in the Cleveland Basin (Yorkshire, UK), 400 km apart. Our synthesis shows that while the Dorset sediments were deposited in an energetically more dynamic setting than the Yorkshire sediments, the overarching climatic and oceanographical processes responsible for variations in organic carbon enrichment and sedimentation were similar. Intervals of coeval organic carbon-rich sedimentation occurred in both basins, and a particulate shuttle was intermittently active in both basins. Consistent with recent climate simulations, we conclude that tropical climate conditions, associated with enhanced nutrient supply, were key drivers of sedimentation between the Jurassic Wessex and Cleveland Basins.

Supplementary material: Geochemical data discussed in the manuscript is available at: https://doi.org/10.6084/m9.figshare.c.4531532

Received 4 March 2019; **revised** 3 June 2019; **accepted** 3 June 2019

Deposition of organic carbon-rich muds has occurred in epicontinental seaways intermittently since at least the onset of the Paleozoic (Negri *et al.* 2009; Schieber 2016). These seaways, often termed continental interior or epeiric seas, are vast, shallow (<100 m), partially enclosed seaways that form as a result of high sea level flooding low lying, flat continental areas (Shaw 1964; Schieber 2016; Kemp *et al.* 2018). Much of what is known about deposition in epicontinental seaways is derived from rock records due to a lack of an appropriate modern-day analogue (Arthur & Sageman 1994). Many of the world's hydrocarbon source rocks were deposited in these settings making them of economic importance. This, along with their 'completeness of record', has sparked a strong interest in the correlation of these deposits across vast distances, and in the processes responsible for their formation (Schieber 2016).

Flooding of low-lying continental areas occurs when global sea level is high during periods when the Earth is under greenhouse conditions and there are no or only small polar ice caps. However, maximum water depths are not thought to have exceeded 10s of metres across most epicontinental seaways in geological time (Shaw 1964; Schieber 2016). Another consequence of greenhouse conditions is an enhanced hydrological cycle (Sellwood & Valdes 2008), where precipitation, and consequently weathering and erosion are intense. This can lead to the delivery of high amounts of freshwater to the oceans from the surrounding land masses. Given the positioning of epicontinental seaways in intracontinental settings, nutrient supply from land is abundant and supports particularly high primary productivity. In addition, the development of salinity stratification due to the formation of a surface freshwater layer can limit vertical exchange processes in the water column. This combination of shallow, stratified, warm seas and plentiful nutrient supply provides ideal conditions for the production of organic material and its export to the seafloor. High primary productivity, coupled with sluggish ocean circulation and limited vertical mixing, leads to oxygen depletion in the bottom waters and creates favourable conditions for the preservation of organic material.

Deposited across the Laurasian Seaway (Fig. 1) during the Kimmeridgian–Tithonian stages of the Late Jurassic, the Kimmeridge Clay Formation (KCF) is a laterally extensive succession, mainly comprising intercalated mudstones and siltstones (Armstrong *et al.* 2016). Organic carbon-rich sediments equivalent in age to the KCF are known as the Draupne and Mandal Formations in the North Sea (Dalland *et al.* 1988), the Spekk Formation in the Norwegian Sea; the Hekkingen Formation in the Barents Sea; and the Agardhfjellet Formation on Svalbard (Hammer *et al.* 2012; Koevoets *et al.* 2016, 2018; Turner *et al.* 2019). Time-equivalent organic carbon-rich successions can be found across the world e.g. in Canada (the Egret Member; Huang *et al.* 1994), Nepal (the Spiti Shales; Pathak 2007), Portugal (the Tojeira Shales; Turner *et al.* 2017), Russia and Siberia (Kashpir Oil Shales; Riboulleau *et al.* 2000), Saudi Arabia (the Hanifa Formation; Moshrif 1984), the USA (Haynesvilles Shale; Hammes *et al.* 2011) and Yemen (the Madbi Formation; Hakimi *et al.* 2010). The KCF exhibits multiscale cyclicity ranging from micron-scale heterogeneity, interpreted to represent annual seasonality in coccolith productivity (Lees *et al.* 2004), to metre- and decimetre-scale cyclicity interpreted to represent orbitally forced shifts in water column stability and

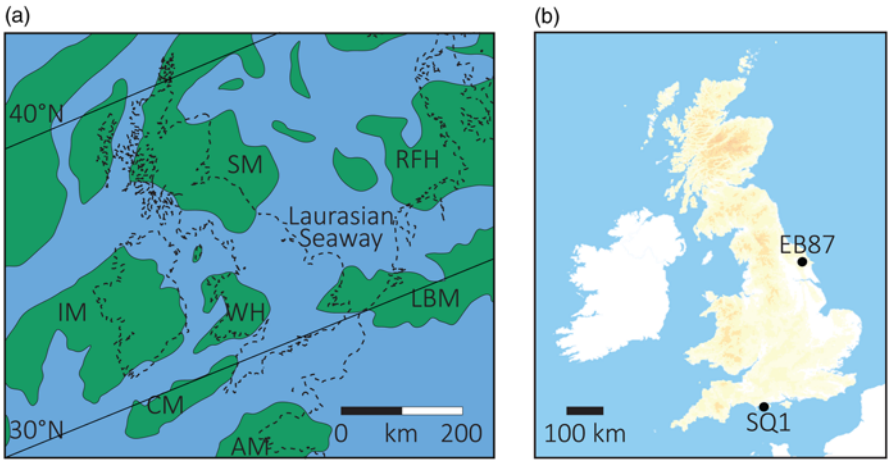

Fig. 1. (**a**) Palaeogeographical map of the Laurasian Seaway modified after Turner *et al.* (2019), where green denotes land and blue denotes sea. Palaeo-landmasses are labelled as follows: IM, Irish Massif; LBM, London–Brabant Massif; RHV, Ringkøbing–Fyn High; AM, Armorican Massif; SM, Scottish Massif; WH, Welsh High; CM, Cornubia Massif. The dashed black lines mark the outline of the modern-day landmasses. (**b**) Map of the modern-day UK showing the locations of the SQ1 (5 0°36′ 13.0″N 2°02′50.0″W) and EB87 (54°12′ 47.7″N 0°37′22.7″W) Cores from Geological Map Data BGS © UKRI 2019.

nutrient supply through continental precipitation (Waterhouse 1999; Morgans-Bell *et al.* 2001; Weedon *et al.* 2004). The KCF has been correlated using ammonite biostratigraphy between the Wessex (Dorset, UK) and Cleveland (Yorkshire, UK) Basins (Gallois 1979; Gallois & Medd 1979; Cox & Gallois 1981; Herbin & Geyssant 1993; Herbin *et al.* 1993, 1995). Organic carbon enrichment occurs in five distinct intervals (Herbin *et al.* 1991) that are termed organic rich belts (ORBs) by Cox & Gallois (1981). Armstrong *et al.* (2016) paired geochemical and sedimentological data with global climate modelling and suggested that the ORBs of the Kimmeridge Clay Formation were deposited under the influence of an expanded Hadley Cell with orbitally modulated northwards shifts of the Intertropical Convergence Zone (ITCZ), which promoted enhanced organic carbon production and preservation in the UK sector of the KCF through elevated continental precipitation and runoff rates.

Here we present new major and trace element records for ORBs 4 and 5 from the Swanworth Quarry 1 Core drilled in the Wessex Basin (Dorset, UK). We compare these data to a recently published equivalent dataset for the coeval succession in the Ebberston 87 Core (Atar *et al.* 2019) drilled in the Cleveland Basin (Yorkshire, UK). We also compare petrographic analyses for ORB 4 from the coastal outcrop in the Wessex Basin (Macquaker & Gawthorpe 1993; Macquaker *et al.* 2010; Lazar *et al.* 2015) to the Ebberston 87 Core (Atar *et al.* 2019). We look beyond the traditional total organic carbon (TOC) and biostratigraphic correlation to explore the extent to which large-scale environmental processes influenced sedimentation generally, and organic matter preservation specifically, across the UK sector of the Laurasian Seaway in the Late Jurassic.

Material and methods

The Swanworth Quarry 1 (SQ1) Core was drilled in the Wessex Basin (Fig. 1) as part of the Natural Environment Research Council's Rapid Global Geological Events (RGGE) special topic 'Anatomy of a Source Rock' project (Gallois 1998, 2000; Wignall & Newton 1998; Chambers *et al.* 2000; Brereton *et al.* 2001; Morgans-Bell *et al.* 2001; Raiswell *et al.* 2001; Lees *et al.* 2004; Pearson *et al.* 2004; Tyson 2004; Pancost *et al.* 2005; Hesselbo *et al.* 2009), and is stored at the British Geological Survey (BGS) Core Store (Keyworth, UK). A total of 172 samples were collected at 50 cm intervals across a *c.* 79 m section (181.42–260.05 metres below surface). The Ebberston 87 (EB87) Core was drilled in the Cleveland Basin as part of a joint project between the BGS and IFP Energies Nouvelles (IFPEN) in 1987 (Herbin *et al.* 1991). The core is stored at the IFPEN facilities (Chartres, France), and a total of 116 samples were collected from the EB87 Core at 50 cm intervals across a *c.* 20 m section (31.07–72.00 metres below surface). Both cores were sampled from the upper *Pectinatites wheatleyensis* to the lower *Pectinatites pectinatus* ammonite zones, which are Tithonian in age.

Samples were powdered to a *c.* 10 μm grain size using an agate Retsch, RS200, Vibratory Disc Mill. Total organic carbon contents were measured after decalcification in hot (60–70°C) 12.5 M HCl using a LECO CS230 Carbon–Sulphur analyser at Newcastle University. Accuracy was measured to 0.08% for total carbon (TC) and 0.14% for TOC calculated to a reference soil. Wavelength-Dispersive X-Ray Fluorescence (XRF) analyses were conducted at the ICBM (University of Oldenburg) to determine the contents of selected major (Si, Al, Ti and Fe) and trace (Mn, As, Co, Cr, Cu, Mo, V, U, Zn and Zr) elements. Borate glass beads were produced by fusing 0.7 g of sample with 4.2 g of $Li_2B_4O_7$ following a pre-oxidation procedure with 1.0 g of $(NH_4)_2NO_3$ in a platinum crucible and measured using a Panalytical Axios Max WD-XRF spectrometer. Calibration including line overlap correction and matrix correction was based on 66 international reference samples. Trueness was checked by international and in-house reference samples not included in the calibration with an error of <3% for major elements and <9% for trace elements (except elements below quantitation limit). Precision was measured at <0.5% for major elements and <7% for trace elements, excluding U for which precision was measured at 16%. Major and trace elements are reported as wt % and ppm, respectively.

Mo and U enrichment factors (EFs; Brumsack 2006) were calculated relative to post-Archean average shale (PAAS; Taylor & McLennan 2001), after Algeo & Tribovillard (2009).

Results

Geochemical results are discussed with reference to the ORBs first described by Cox & Gallois (1981). Based on the established chronostratigraphic framework, in the SQ1 Core, ORB 4 is 20.5 m thick and spans 230.00–250.50 metres below surface (mbs) and ORB 5 is 30.5 m thick and spans 178.5–209.00 mbs (Fig. 2). The EB87 Core is a more condensed section relative to the SQ1 core. In the EB87 Core, ORB 4 is 11.5 metres thick and spans 63.00–74.50 mbs and ORB 5 is 18 metres thick and spans 32.5–50.50 mbs (Fig. 2). Note that in the SQ1 Core, not the entire section of ORB 4 and 5 is analysed due to sampling.

In the SQ1 Core, TOC contents in ORB 4 range from 1.3–38.2 wt %, with a mean of 5.2 wt % (Fig. 3). In ORB 5, TOC contents range from 2.9–42.6 wt %, with a mean of 10.3 wt % (Fig. 3) and between ORBs 4 and 5, TOC is markedly lower, ranging from 0.2–5.7 wt %, with a mean of 1.9 wt % (Fig. 3). In the EB87 Core, TOC ranges from 2.8–20.7, with a mean of 9.5 wt % in ORB 4. In ORB 5 of the EB87 Core, TOC ranges from 2.8–25.7 wt %, with a mean of 8.8 wt %. In between ORBs 4 and 5, TOC ranges from 0.8–6.4 wt %, with a mean of 2.4 wt % (Fig. 3).

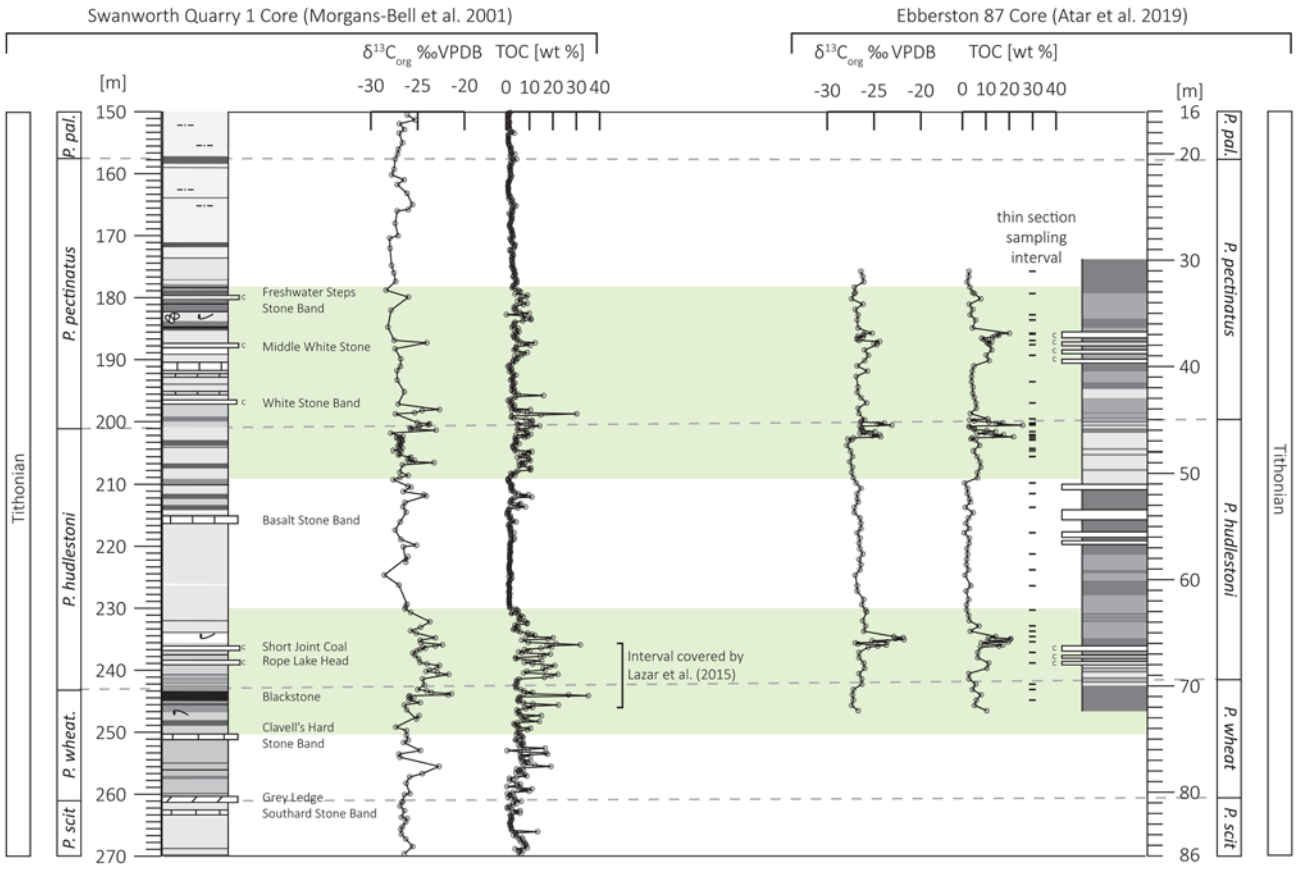

Fig. 2. Correlation panel between the Swanworth Quarry 1 (SQ1) Core from the Wessex Basin (Dorset, UK) and Ebberston 87 Core from the Cleveland Basin (Yorkshire, UK). Depths are in metres below surface. Graphic log, total organic carbon (TOC), and organic carbon isotope ($\delta^{13}C_{org}$) data for the SQ1 Core are from Morgans-Bell *et al.* (2001). Lithology is with Munsell Colour. Graphic log for the EB87 Core is from IFPEN archives, and total organic carbon (TOC) and organic carbon isotope ($\delta^{13}C_{org}$) data is from Atar *et al.* (2019). Colour is based on drilling descriptions. Horizontal dashed lines mark biostratigraphical zonation ties. Green panels depict ORBs 4 (lowermost) and 5 (uppermost) defined by Cox & Gallois (1981). Interval over which detailed petrographical study was conducted in Lazar *et al.* (2015) is marked on the SQ1 depth scale.

Figure 4 shows contents of Al_2O_3, CaO and SiO_2 in all analysed samples, which represent the main sediment components: clay, carbonate and quartz or biogenic silica, respectively. Samples from the SQ1 Core plot along a mixing line between carbonate and average shale (Wedepohl 1991) end-members, whereas samples from the EB87 Core plot along a mixing line between carbonate and a detrital end-member that is more Al-rich than average shale. Al-normalized values of Si, Ti and Zr can be used as grain size indicators, and Al-normalized K and Rb can be used as weathering and sediment provenance indicators (e.g. Sageman *et al.* 2003; Brumsack 2006; Grygar *et al.* 2019). Aluminium-normalized Si, Ti, Zr, K and Rb range from 2.0–3.8, 0.04–0.07, 8.2–33.2, 0.2–0.3 and 16.5–24.0 in ORB 4, respectively (Fig. 5). In ORB 5, they range from 2.0–4.1, 0.05–0.07, 12.2–34.7, 0.2–0.3 and 13.2–20.0, respectively (Fig. 5). However, in between the ORBs, they are less variable, ranging from 2.2–2.8, 0.05–0.06, 11.1–19.4, 0.3–0.4 and 18.6–20.1, respectively (Fig. 5).

In ORB 4 of the EB87 Core, Al-normalized Si, Ti, Zr, K and Rb range from 2.1–2.6, 0.05–0.06, 10.4–18.0, 0.2–0.3and 10.1–17.0, respectively. In ORB 5, Al-normalized Si, Ti, Zr, K and Rb range from 2.0–3.3, 0.04–0.05, 9.8–26.7, 0.1–0.3 and 8.6–17.6, respectively. As in the SQ1 Core, in between ORBs 4 and 5, the Al-normalized Si, Ti, Zr, K and Rb are lower and much less variable, ranging from 2.0–2.4, 0.05–0.05, 11.0–14.0, 0.2–0.3 and 12.0–17.0, respectively. In ORB 5, Ti/Al, Zr/Al and Rb/Al are generally the same or exceed average shale values in the SQ1 Core, but the values are below average in the EB87 Core (Fig. 5). Si/Al and K/Al are generally below average shale values for both cores in ORB 5 (Fig. 5). For ORB 4, values of Si/Al, Ti/Al. Zr/Al and K/Al are generally less than average shale in both cores (Fig. 5). In ORB 4, Rb/Al is higher than average shale in the SQ1 core but lower in the EB87 Core (Fig. 5). Generally, Al-normalized Si, Ti, Zr and K are about the same or lower than average shale between ORBs 4 and 5 in both cores (Fig. 5). Conversely, Rb/Al is higher than average shale in SQ1 and around average shale in EB87 in between ORBs 4 and 5 (Fig. 5).

Each trace element has a unique sensitivity to ambient redox conditions and affinity to organic matter or hydrogen sulphide, and application of these trace metal proxies enables us to reconstruct palaeo-redox conditions. In this study, we are specifically concerned with the application of these proxies but we refer to (Brumsack 2006; Tribovillard *et al.* 2006; Calvert & Pedersen 2007) for further details and discussion on trace element sequestration. In both the SQ1 and the EB87 Cores, the Al-normalized ratios of the redox-sensitive elements (Fe, Mn, As, Cu, Mo, U, V and Zn) are generally higher and more variable within ORBs 4 and 5 but are generally lower and markedly more uniform in between the ORBs (Fig. 6). However, the baseline values in EB87 are slightly higher than in the SQ1 Core. See supplementary information for data tables. Figure 7 shows a crossplot of molybdenum and uranium enrichment factors calculated to relative to post-Archean average shale (PAAS; Taylor & McLennan 2001, after Tribovillard *et al.* 2012).

Linear sedimentation rates (LSRs) were calculated for the *P. wheatleyensis*, *P. hudlestoni*, and *P. pectinatus* biozones for both cores using ammonite zonal boundary dates in the geological timescale (Gradstein *et al.* 2012). For the SQ1 Core, the LSRs were 10.1, 9.0 and 7.3 cm/ky, respectively. For the EB87 Core, the LSRs were 6.6, 5.1 and 4.1 cm/ky for each biozone, respectively.

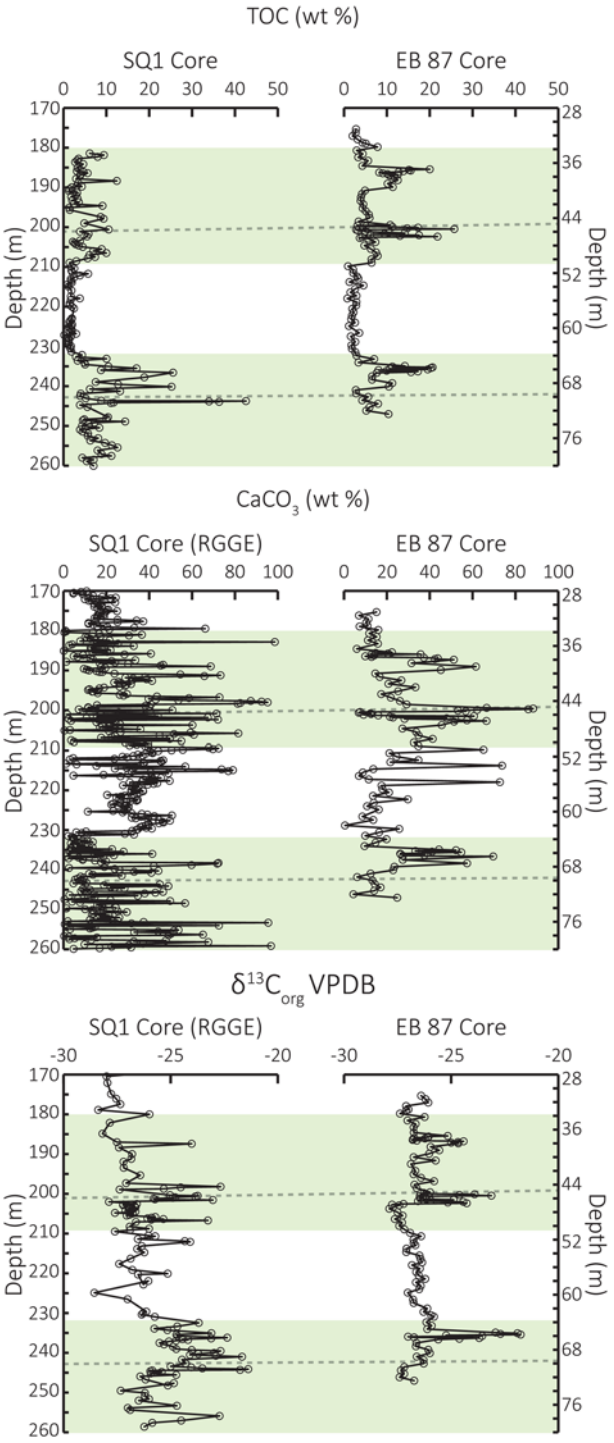

Fig. 3. Total organic carbon (TOC), calcium carbonate ($CaCO_3$) and organic carbon isotopes values ($\delta^{13}C_{org}$) for the Swanworth Quarry 1 (SQ1) and Ebberston 87 (EB87) Cores. Depths are in metres below surface. Horizontal dashed lines mark biostratigraphical zonation ties. Green panels depict ORBs 4 (lowermost) and 5 (uppermost) defined by Cox & Gallois (1981). $CaCO_3$ and $\delta^{13}C_{org}$ for the SQ1 core is from Morgans-Bell *et al.* (2001). TOC, $CaCO_3$ and $\delta^{13}C_{org}$ data from the EB87 Core is from Atar *et al.* (2019).

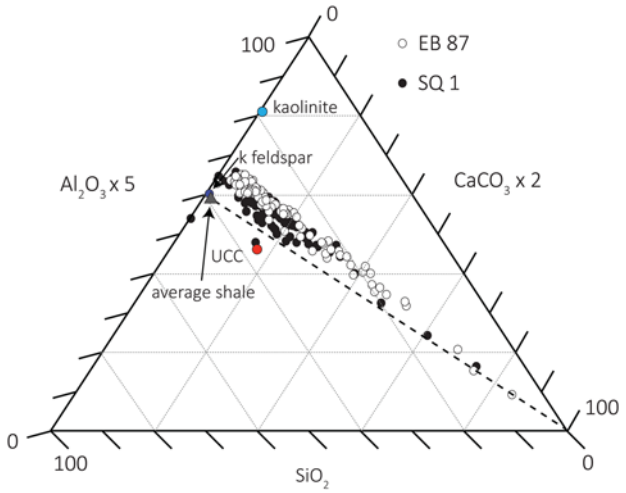

Fig. 4. Ternary diagram (Brumsack 1989) displaying the relative contributions of clay (Al_2O_3), quartz/biogenic silica (SiO_2) and carbonate ($CaCO_3$) of all samples. Black and white circles depict the SQ1 and EB87 data, respectively. Axes are scaled to improve display of the data. Average shale (Wedepohl 1991), upper continental crust (UCC; Rudnick & Gao (2003)), K-feldspar and kaolinite are plotted for reference. Dashed line shows the average shale–carbonate mixing line.

Discussion

Depositional controls in the UK Wessex and Cleveland Basins

In the Cleveland and Wessex Basins, ORB 4 comprises a mixture of detrital material, carbonate and marine organic material. The detrital fraction constitutes of sub-rounded quartz, feldspar, and titanium oxide grains, the clay minerals illite and kaolinite (which is partly authigenic and infilling foraminifera tests), and terrestrial Type III organic material (Macquaker & Gawthorpe 1993; Lazar *et al.* 2015; Atar *et al.* 2019). Authigenic kaolinite infills foraminifera tests in both sections (Macquaker & Gawthorpe 1993; Atar *et al.* 2019). Carbonate is present as pristinely preserved coccoliths, foraminifera, calcispheres and rhombohedral dolomite (Macquaker & Gawthorpe 1993; Lazar *et al.* 2015; Atar *et al.* 2019). The former three carbonate components are biological and formed in the ocean whereas the dolomite crystals are post-depositional and therefore do not reflect primary depositional conditions. The geochemical characterization of the main constituents of the SQ1 and EB87 Cores is illustrated by the SiO_2, Al_2O_3 and CaO ternary plot (Fig. 4), where SiO_2 represents quartz and/or biogenic silica, Al_2O_3 denotes clay and CaO indicates carbonate (after Brumsack 1989). The higher degree of scatter for the SQ1 core samples indicates an overall more heterogeneous lithology than in the EB87 Core (Fig. 4). Samples that plot above the mixing line towards higher Al_2O_3 fractions may indicate either a higher degree of chemical weathering or a higher clay to quartz (or biogenic silica) ratio.

Petrographic observations of wispy algal macerals and high $\delta^{13}C_{org}$ values (Fig. 3) in the EB87 Core indicate that the dominant source of carbon in ORBs 4 and 5 is Type II marine organic material deposited as marine snow and/or algal mats. In between the ORBs, the organic material occurs as equant lumps and lower $\delta^{13}C_{org}$ indicate a more dominant Type III terrestrial organic matter source. Microcycles within organic matter type and TOC contents identified within the EB87 Core (Herbin *et al.* 1993; Boussafir *et al.* 1995) support the change in dominant organic matter type in the ORBs and between them. The isotope trends in the SQ1 Core are similar to that of the EB87 Core, in that they are more positive in the ORBs than in the intervals between. We interpret this to indicate shifts in the dominant sources of organic carbon between the ORBs and intercalated sediments in the SQ1 Core. The changes in organic material type throughout both sections (Fig. 3) suggest higher primary productivity during deposition of the ORBs, which may have resulted from mixing of the water column associated with higher depositional energies, higher nutrient supply from enhanced continental weathering, or both, which is supported by organic geochemical analyses (Ramanampisoa & Disnar 1994). It has been proposed that a productivity-driven mechanism, established for an underlying ORB in the Cleveland

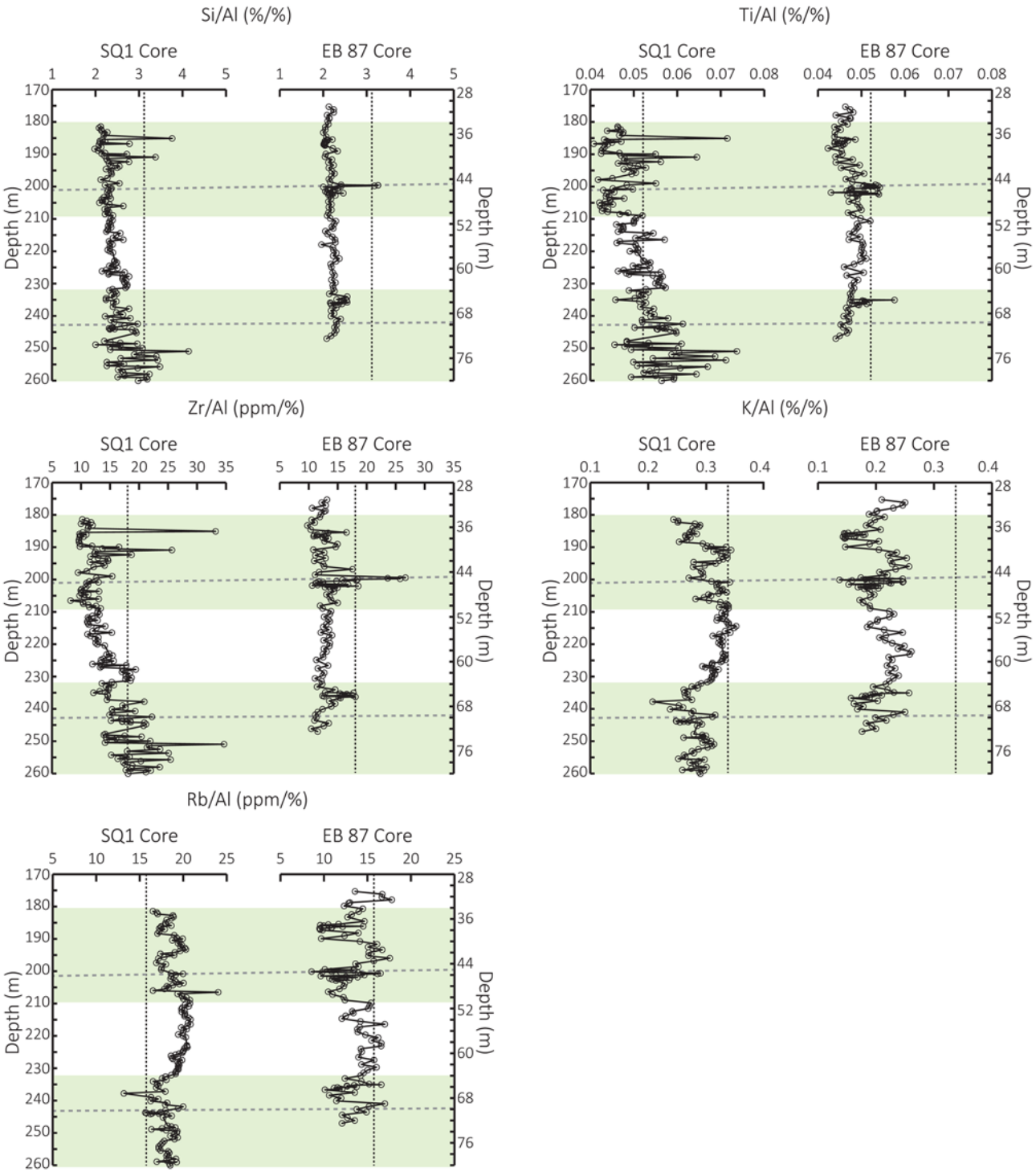

Fig. 5. Depth plots of depositional energy and continental weathering indicators (Al-normalized Si, Ti, Zr, K and Rb) for the Swanworth Quarry 1 and Ebberston 87 Cores. For the Si/Al, Ti/Al and Zr/Al grain size or depositional energy increase towards the right. Vertical dashed lines indicate average shale values (Wedepohl 1991). Depths are in metres below surface. Horizontal dashed lines mark biostratigraphical zonation ties. Green panels depict ORBs 4 (lowermost) and 5 (uppermost) defined by Cox & Gallois (1981). Data for the Ebberston 87 Core is from Atar *et al.* (2019).

Basin (Tribovillard *et al.* 1994), may have controlled organic carbon cyclicity through the entire KCF (Tribovillard *et al.* 2004). Enhanced productivity and/or burial of organic carbon may also contribute to the observed shifts in carbon isotope values as was suggested for lower in the KCF (Zuo *et al.* 2018). Another option is stratification of the water column resulting in a more anoxic/euxinic lower water column which enhances the preservation of organic carbon at the sediment/water interface. It has also been suggested that organic matter sulphurization enhanced preservation in the Cleveland Basin (Lallier-Vergès *et al.* 1993, 1997; Boussafir & Lallier-Vergès 1997).

As expected, the terrigenous components in both cores decrease as the biogenic components increase (Fig. 3). The terrigenous components may be diluted by the biological components at times of high productivity. Alternatively, the lower detrital contents in the ORBs may represent times where the supply of detrital material dwindled. However, distance from the terrigenous sediment source is difficult to constrain in an epicontinental seaway due to low bathymetric gradients, imprecise estimations of water depths, palaeogeographical reconstructions (Schieber 2016) and only weakly constrained fluctuations of bulk sedimentation and

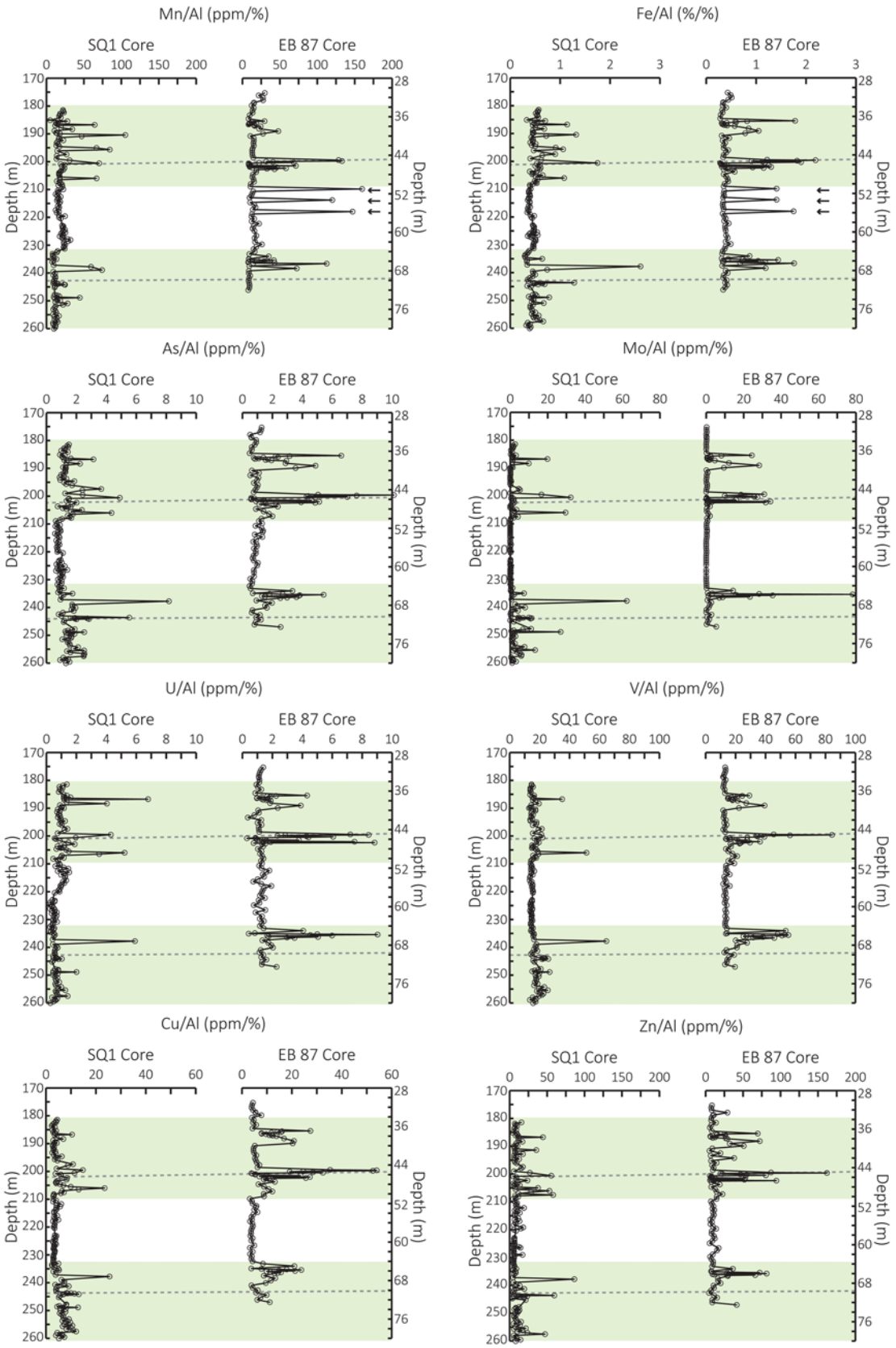

Fig. 6. Depth plots of redox indicators (Al-normalized Mn, Fe, As, Mo, U, V, Cu and Zn) for the Swanworth Quarry 1 and Ebberston 87 Cores. Depths are in metres below surface. Horizontal dashed lines mark biostratigraphical zonation ties. Vertical dashed lines indicate average shale values (Wedepohl 1991). Green panels depict ORBs 4 (lowermost) and 5 (uppermost) defined by Cox & Gallois (1981). Data for the Ebberston 87 core is from Atar *et al.* (2019).

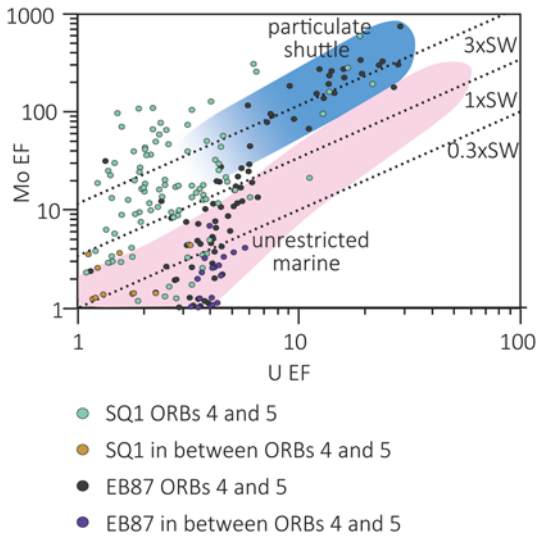

Fig. 7. Plot of Mo EF against U EF calculated relative to post-Archean average shale (PAAS; Taylor & McLennan 2001; after Tribovillard *et al.* 2012). Samples from ORBs 4 and 5 from the SQ1 and EB87 Cores are indicated by pale green circles and dark grey circles, respectively. Samples in between the ORBs in the SQ1 and EB87 cores are depicted by orange circles and purple circles, respectively. Dashed lines are modern day seawater, 0.3× modern day seawater and 0.1× modern day seawater values shown for reference. The particulate shuttle is mapped in blue and unrestricted marine setting is mapped in pink. Axes are logarithmic.

compound accumulation rates. Based on these limitations we conclude that it is not possible to confidently discern these control mechanisms with the present dataset.

Depth plots of geochemical indicators at both sites for coarser grain sizes/higher amounts of heavy minerals (Fig. 5; Al-normalized Si, Ti and Zr; (Schnetger *et al.* 2000) are generally lower than average shale. However, the site of deposition of SQ1 in the Wessex Basin had overall higher, but also more variable, energetic conditions during the deposition of the ORBs (Fig. 8). Quartz (Si) and heavy mineral enrichment (zircon, Ti-minerals) can occur either by a winnowing effect due to a higher depositional energy as a result of stronger ocean currents or by a preferential transport of these minerals due to a higher wind strength on the continent. The same indicators are lower in the sediment deposited in between the ORBs, consistent with deposition of finer-grained sediment under more quiescent conditions. By contrast, depositional energy indicators are consistently lower in EB87 than in SQ1 (Fig. 5), supporting the interpretation of the ternary diagram where all samples are richer in Al and poorer in Si in EB87 than in SQ1 (Fig. 5). Relative enrichments of Al-normalized Si, Ti and Zr ratios within the ORBs (Fig. 5) suggest that depositional energies were elevated and variable during deposition of these intervals in both the Cleveland and Wessex Basins, which is further supported by petrographic evidence of normally-graded erosional beds of ORB 4. The higher energy and coarser grain sizes in the Wessex Basin may result from winnowing of the sediment by bottom currents and/or wave activity reaching the seafloor (Fig. 8).

In contrast to the coarse grain size-/heavy mineral-bound elements Si, Ti and Zr, the abundance of K and Rb in marine sedimentary rocks is related to sediment provenance and/or weathering rates on the adjacent sediment because they are (like Al) commonly associated with fine-grained/lower-density terrigenous minerals like K-feldspar and clay minerals (Calvert & Pedersen 2007; Grygar *et al.* 2019). Sediment routing systems and weathering rates are both affected by climate-driven processes, so K/Al and Rb/Al ratios can be used to infer changes in climatic conditions and processes on landmasses adjacent to depositional basins. The similarity between these ratios in both cores (Fig. 5) therefore indicates the same overarching processes being responsible for their down-core patterns in both the Wessex and the Cleveland Basins.

While the elements/proxies discussed so far behave biogeochemically conservatively and are mainly affected by physical processes in the depositional environment (except for K and Rb), selected trace elements behave differently under different redox conditions. In general, most redox-sensitive/sulphide-forming trace elements (e.g. As, Mo, U, V, Cu and Zn) are enriched under anoxic (oxygen-free) to euxinic (anoxic and sulphidic) sediment pore and bottom water conditions. This is due to several mechanisms, including association of the trace elements to organic material and formation of sulphide minerals (Brumsack 2006; Tribovillard *et al.* 2006; Calvert & Pedersen 2007). Generally, during low oxygen depositional conditions, Mn is depleted, whereas under oxic conditions Mn/Al in ocean sediments is close to average shale or above (Brumsack 2006). Relatively low values of Mn/Al (Fig. 6) indicate sediment pore waters were suboxic for most of the deposition of both successions. Repeated enrichments compared the average shale level of redox-sensitive/sulphide-forming trace elements (As, Mo, U, V, Cu and Zn: Fig. 6) in line with a depletion in Mn within the ORBs demonstrate that pore- and bottom- water conditions were anoxic to euxinic, at least episodically, in both the Wessex and Cleveland Basins. This is supported by organic carbon enrichments as its preservation is enhanced by an absence of oxygen and the presence of hydrogen sulphide at the seafloor. Intermittent euxinia in the sediment pore waters in the Wessex Basin is supported by palaeontological (Wignall & Myers 1988), geochemical (Van Kaam-Peters *et al.* 1998; Sælen *et al.* 2000; Raiswell *et al.* 2001) and pyrite framboid size (Wignall & Newton 1998) analyses. However, values approaching average shale for the Mn/Al ratio within the ORBs in both sections and parallel low element/Al ratios of redox-sensitive/sulphide-forming trace elements (As, Mo, U, V, Cu and Zn) indicate repeated phases of oxic bottom water conditions (Fig. 8). In the EB87 Core, such oxic incursions are supported by petrographic evidence that reveals co-occurrence between relatively elevated Mn contents, agglutinated foraminifera and pristinely preserved carbonate (coccolith) material (Atar *et al.* 2019). Repeated fluctuations between oxic and anoxic/euxinic redox conditions may result from storm activity mixing and ventilating the water column as evidenced by normally graded beds with erosional bases within the ORBs, which point towards the remobilization and lateral transport of sediment (Lazar *et al.* 2015). Tribovillard *et al.* (2019) recently proposed a mechanism whereby storm activity concentrated sulphurised, marine-origin organic matter in shallow marine environments, which may be applicable to organic matter enrichment in the Wessex and Cleveland Basins.

In the interval between ORBs 4 and 5, both cores exhibit much less variation, representing overall more stable redox conditions. The low concentrations of redox sensitive/sulphide-forming trace elements (Fig. 6) and TOC (Fig. 3), along with slightly elevated Mn/Al values (Fig. 6), support that the bottom waters of the Wessex Basin were suboxic during this interval. By contrast, in the correlative interval in EB87, As and U are slightly enriched and Mn is low (Fig. 6), suggesting that pore waters were suboxic-anoxic in the Cleveland Basin (Fig. 8). Active bottom water currents/wave action, as previously indicated by Si/Al, Ti/Al and Zr/Al ratios, would have increased bottom water ventilation, which may account for the suboxic bottom water conditions observed in the Wessex Basin between the ORBs.

The particulate shuttle is significant in the transfer of trace metals from the water column to the sediment in some depositional settings (Goldberg 1954; Algeo & Tribovillard 2009; Tribovillard *et al.* 2015). Tribovillard *et al.* (2015) use Mo, As and Sb as proxies for the presence of an Fe–Mn particulate shuttle, which involves the oxidation of Mn^{2+} and Fe^{2+} to form (oxyhydr)oxides in the surface

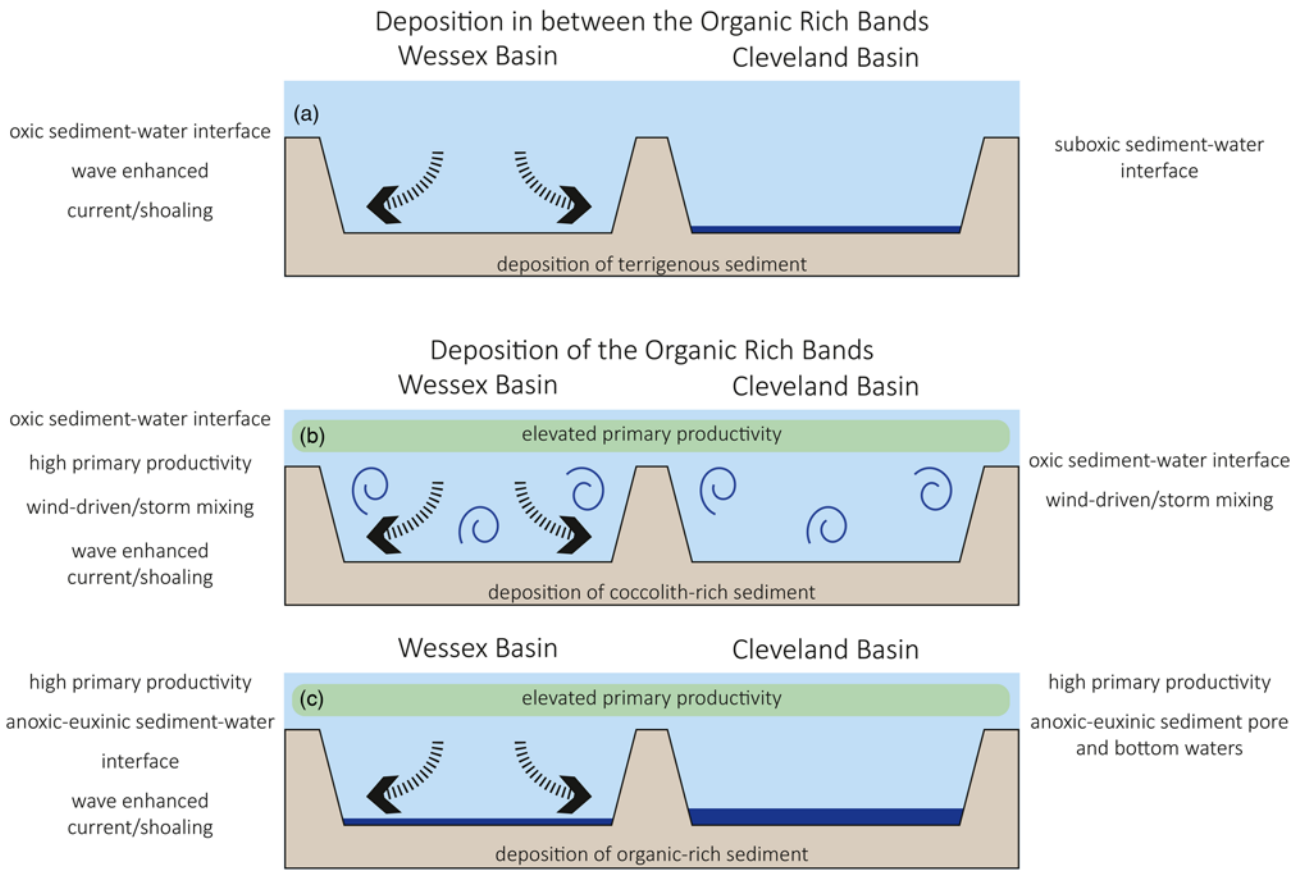

Fig. 8. Schematic diagram showing the differences between the Wessex and Cleveland Basins during the deposition of the ORBs and the interval in between. Black dashed arrows denote the presence of bottom currents/shoaling.

waters, adsorption of trace elements to the (oxyhydr)oxides, and the subsequent export to deeper waters. In anoxic–euxinic settings, the (oxyhydr)oxides are reduced, the Mn^{2+} diffuses back to the surface waters, and the Fe^{2+} reacts to form Fe sulphide minerals (e.g. pyrite) (Canfield *et al.* 1992; Huckriede & Meischner 1996; Neretin *et al.* 2004; Dellwig *et al.* 2010). Atar *et al.* (2019) concluded that a Mn–Fe particulate shuttle was intermittently active in the Cleveland Basin during the deposition of the ORBs (Fig. 7). The SQ1 data (Fig. 7) show that a particulate shuttle was also active intermittently during deposition of the ORBs, but that suboxic conditions were likely limited to the sediment pore waters during deposition in between the ORBs in the Wessex Basin.

Pertinent to assessing interconnectivity of sub-basins within an epicontinental seaway is the relative degree of water-mass restriction within each of these sub-basins. Trace element ratios, specifically Mo and U, can be used to assess hydrographic restriction of a basin because of their respective redox behaviours (Algeo & Tribovillard 2009) (Fig. 7). Molybdenum is quantitatively removed from the water column under moderately to strongly euxinic conditions, much more so than U. Conversely, under suboxic conditions, U is likely to be enriched as it becomes trapped at the Fe(II)/Fe(III) redox boundary (Algeo & Tribovillard 2009; Tribovillard *et al.* 2012). Atar *et al.* (2019) concluded that the Cleveland Basin was unlikely to have been restricted for prolonged periods of time, if at all. This agreed with previous studies that concluded prolonged restriction of the Wessex Basin was also unlikely (Pearce *et al.* 2010; Tribovillard *et al.* 2012). Data from this study (Fig. 7) also align with this: high enrichments of Mo relative to U indicate intermittently strongly euxinic conditions during the deposition of the ORBs in the Wessex Basin. Such enrichments would have required a connected water mass to resupply the Mo, which is indicated by values around three times that of seawater (Fig. 7).Overall, our observations align with the hypothesis that sediment deposition in the Laurasian Seaway took place under the influence of tropical conditions that resulted from an expanded or migrated Hadley Cell (Armstrong *et al.* 2016), but see Wignall & Ruffell (1990), Ruffell *et al.* (2002), Hesselbo *et al.* (2009) and Zuo *et al.* (2019) for alternative discussions of climate conditions. We suggest that during the deposition of ORBs 4 and 5, elevated production and preservation of organic carbon was promoted by an enhanced nutrient supply through continental weathering and water column mixing during storm events, which resulted from tropical-like climate conditions. Regional sea level has been reconstructed through the application of sequence stratigraphy to the coastal section in Boulonnais (France) (Herbin *et al.* 1995; Williams *et al.* 2001). Biostratigraphic correlation of the Wessex and Cleveland Basin deposits to the Boulonnais section reveals that ORBs 1–5 do not correlate to fluctuations in sea level, so this cannot be the primary driver of coeval organic carbon variability across the seaway (Herbin *et al.* 1995). Herbin *et al.* (1995) instead concluded that sea level worked in conjunction with overarching climate conditions to facilitate the repeated organic carbon enrichments.

Chemostratigraphic cross-seaway correlation

The use of ammonite biostratigraphy in the correlation of Jurassic deposits across northwest Europe is a well-established method (Jenkyns 2003; Cope 2009). It is most successful when conducted on well-exposed outcrops where the chance of finding specimens is maximized by following laterally extensive beds. This is not the case for drill wells, as the paucity of key species makes the chances of finding an appropriate specimen in a five-centimetre drill core markedly less compared to extensive outcrops. This poses a challenge when conducting high resolution correlations between two biostratigraphically constrained cores, as in this study.

The biostratigraphic ties between the SQ1 and EB87 Cores are marked by grey dashed lines on Figures 2, 3, 5, and 6. As discussed, the geochemical indictors bare a remarkable similarity to one another. However, when considering the geochemical plots relative to the biostratigraphical boundaries, there is a slight offset between the two cores around the *P. hudlestoni* and *P. pectinatus* ammonite zone boundary. This may result from a difference in thickness of the sediment deposited in the two basins, where the EB87 Core may exhibit a more condensed section relative to the SQ1 Core due to a difference in sedimentation rates and processes. Alternatively, the slight offset in geochemical profiles between the two cores may result from diachronous sedimentary processes which would be driven by variations in climate and/or sea level. Further, the fauna used to date these sediments may have migrated temporally, which could lead to an offset between the biostratigraphic ages in the two cores. Finally, the SQ1 Core has been extensively studied so sampling depths of the core may have been disrupted during storage over the past ten years. It is difficult to determine whether or not the observed offset is due to erroneous biostratigraphy through either lack of appropriate specimens or temporal migration of fauna, or whether it records a true offset between environmental conditions, with the present dataset. However, given the slight nature of the offset, and considering the age of the studied sedimentary rocks, the apparent anomaly is not significant enough to discredit the comparison between the two sections.

In an attempt to correlate sections at greater resolution, biostratigraphy was paired with TOC data to correlate five broad bands of organic carbon enrichment across the Wessex and Cleveland Basins; these ORBs occur on a metre to decimetre scale (Gallois 1979). However, TOC data cannot be used to correlate the sections at a higher resolution, i.e. centimetre scale, owing to the labile nature of organic material (Jenkyns *et al.* 2002). Organic material is highly susceptible to degradation in the presence of oxidants, therefore very specific local conditions are required to preserve significant amounts of it. Furthermore, TOC contents are affected by sedimentation rate and primary productivity, both of which are influenced by a range of factors such as nutrient supply and ocean circulation. To mitigate this challenge, ratios of elements with biogeochemically and hydrodynamically conservative behaviour must be used instead. Potassium and rubidium are strong candidates for this as changes in the Al ratios of both elements are dependent upon weathering on adjacent hinterlands (Grygar *et al.* 2019).

Similarities between the Wessex and Cleveland Basins are clear; both settings underwent intervals of enhanced primary productivity and organic matter preservation. In both sections, these intervals were highly dynamic and oscillated between fully oxic to euxinic sediment pore and bottom waters during periods of enhanced depositional energies. However, the grain size indicators (Fig. 5) demonstrate that deposition in the Wessex Basin occurred under much higher energy conditions relative to the Cleveland Basin. Despite this, overarching climate processes are still recognizable in the K/Al and Rb/Al trends of both cores, implying that we can in principle use inorganic geochemical data sets to unpick large-scale climate controls, such as precipitation over adjacent land and across seaways. Clay mineral content can be affected by burial diagenesis; however, Hesselbo *et al* (2009) ruled out the diagenetic overprinting of primary signals in the KCF in the Wessex through the consideration of regional geology, shallow burial depths and RockEval parameters that indicate the sediments are thermally immature. The same can be said for the KCF in the Cleveland Basin, which is also reported thermally immature (Herbin *et al.* 1991). Furthermore, authigenically precipitated kaolinite would still require a source of Al close to the site of precipitation, which can only be another detrital silicate mineral (e.g. feldspar) thus the diagenesis should not affect K/Al or Rb/Al ratios discussed in this study.

Provenance/weathering indicators, specifically K/Al and Rb/Al, are uniform across the UK sector of the Laurasian Seaway and are controlled by the same, large-scale climate factors in both basins. Consequently, the expected/assumed synchronicity between the K/Al and Rb/Al profiles can be used to improve the age model proposed from biostratigraphy. In this instance, chemostratigraphy should complement biostratigraphy, which has been shown to be particularly useful when working with core material (e.g. Turner *et al.* 2016). Furthermore, this provides a robust tool when sedimentation rates are known to differ between depositional settings, and when the application of cyclostratigraphy to the studied sections is not statistically robust due to a limited number of sampled cycles.

Conclusions and implications

- The depositional environment in the Wessex and Cleveland Basins, 400 km apart, were remarkably similar during the Late Jurassic.
- Geochemical and petrographic data agree that depositional energy was more variable and slightly higher in the Wessex Basin than in the Cleveland Basin in ORB 4.
- Redox conditions during deposition of the two sediment intervals were similar in that during the ORBs, both sub-basins experienced fluctuations between oxic and euxinic conditions. However, in the Wessex Basin, the anoxic–euxinic periods were shorter and less sustained than in the Cleveland Basin. The interval between ORBs 4 and 5 was predominantly suboxic in both the Wessex and Cleveland Basins.
- Overarching tropical climate conditions were likely responsible for sedimentation across the UK sector of the Laurasian Seaway in the Late Jurassic.
- Varying element/Al ratios, in this particular study K/Al and Rb/Al ratios, are valuable chemostratigraphic correlation tools in environments with differing depositional energies, in particular when studying drill cores.
- This study demonstrates the value of studying time-equivalent but geographically distant sediment cores when investigating large scale depositional processes, particularly in settings such as epicontinental seaways that exhibit high resolution records.

Acknowledgements We wish to thank staff at the Scottish Universities Environmental Research Centre for use of the facilities and help with sample preparation. Phil Green, Alex Charlton and David Earley are thanked for analytical assistance and training at Newcastle University. Liam Herringhsaw is thanked for assistance in sampling the core.

Funding The work contained in this publication was undertaken during a PhD that was funded by Durham University as part of the Natural Environment Research Council (NERC) Centre for Doctoral Training (CDT) in Oil & Gas [grant number NEM00578X/1], whose support is gratefully acknowledged.

Scientific editing by Yanni Gunnell

References

Algeo, T.J. & Tribovillard, N. 2009. Environmental analysis of paleoceanographic systems based on molybdenum–uranium covariation. *Chemical Geology*, **268**, 211–225, https://doi.org/10.1016/j.chemgeo.2009.09.001

Armstrong, H.A., Wagner, T. *et al.* 2016. Hadley circulation and precipitation changes controlling black shale deposition in the Late Jurassic Boreal Seaway. *Paleoceanography*, **31**, 1041–1053, https://doi.org/10.1002/2015PA002911

Arthur, M.A. & Sageman, B.B. 1994. Marine black shales: depositional mechanisms and environments of ancient deposits. *Annual Review of Earth and Planetary Sciences*, **22**, 499–551, https://doi.org/10.1146/annurev.ea.22.050194.002435

Atar, E., März, C. *et al.* 2019. Dynamic climate-driven controls on the deposition of the Kimmeridge Clay Formation in the Cleveland Basin, Yorkshire, UK.

Climate of the Past Discussion, in review, https://doi.org/10.5194/cp-2018-172

Boussafir, M. & Lallier-Vergès, E. 1997. Accumulation of organic matter in the Kimmeridge Clay Formation (KCF): an update fossilisation model for marine petroleum source-rocks. *Marine and Petroleum Geology*, **14**, 75–83, https://doi.org/10.1016/S0264-8172(96)00050-5

Boussafir, M., Gelin, F., Lallier-Verges, E., Derenne, S., Bertrand, P. & Largeau, C. 1995. Electron microscopy and pyrolysis of kerogens from the Kimmeridge Clay Formation, UK: source organisms, preservation processes, and origin of microcycles. *Geochimica et Cosmochimica Acta*, **59**, 3731–3747, https://doi.org/10.1016/0016-7037(95)00273-3

Brereton, N., Gallois, R. & Whittaker, A. 2001. Enhanced lithological description of a Jurassic mudrock sequence using geophysical wireline logs. *Petroleum Geoscience*, **7**, 315–320, https://doi.org/10.1144/petgeo.7.3.315

Brumsack, H. 1989. Geochemistry of recent TOC-rich sediments from the Gulf of California and the Black Sea. *Geologische Rundschau*, **78**, 851–882, https://doi.org/10.1007/BF01829327

Brumsack, H. 2006. The trace metal content of recent organic carbon-rich sediments: implications for Cretaceous black shale formation. *Palaeogeography, Palaeoclimatology, Palaeoecology*, **232**, 344–361, https://doi.org/10.1016/j.palaeo.2005.05.011

Calvert, S.E. & Pedersen, T.F. 2007. Chapter Fourteen Elemental Proxies for Palaeoclimatic and Palaeoceanographic Variability in Marine Sediments: Interpretation and Application. *In*: Claude, H.M. & Anne De, V. (eds) *Developments in Marine Geology*. Elsevier, Amsterdam, 567–644.

Canfield, D.E., Raiswell, R. & Bottrell, S.H. 1992. The reactivity of sedimentary iron minerals toward sulfide. *American Journal of Science*, **292**, 659–683, https://doi.org/10.2475/ajs.292.9.659

Chambers, M., Lawrence, D., Sellwood, B. & Parker, A. 2000. Annual layering in the Upper Jurassic Kimmeridge Clay Formation, UK, quantified using an ultra-high resolution SEM-EDX investigation. *Sedimentary Geology*, **137**, 9–23, https://doi.org/10.1016/S0037-0738(00)00092-0

Cope, J. 2009. Correlation problems in the Kimmeridge Clay Formation (Upper Jurassic, UK): lithostratigraphy versus biostratigraphy and chronostratigraphy. *Geological Magazine*, **146**, 266–275, https://doi.org/10.1017/S0016756808005852

Cox, B.M. & Gallois, R.W. 1981. The stratigraphy of the Kimmeridge Clay of the Dorset type area and its correlation with some other Kimmeridgian sequences. *Institute of Geological Sciences, Natural Environment Research Council*, **1981**, 41.

Dalland, A., Worsley, D. & Ofstad, K. 1988. A lithostratigraphic scheme for the Mesozoic and Cenozoic succession offshore mid- and northern Norway. *NPD-Bulletin*, **4**, 65.

Dellwig, O., Leipe, T. *et al.* 2010. A new particulate Mn–Fe–P-shuttle at the redoxcline of anoxic basins. *Geochimica et Cosmochimica Acta*, **74**, 7100–7115, https://doi.org/10.1016/j.gca.2010.09.017

Gallois, R. 1979. *Oil shale resources in Great Britain*. Institute of Geological Sciences, London, 2.

Gallois, R. 1998. *The stratigraphy of well-completion reports for the Swanworth Quarry No. 1 and No. 2 and Metherhills No. 1 boreholes (RGGE Project), Dorset*. *British Geological Survey Technical Report WA/97/91*.

Gallois, R. 2000. The stratigraphy of the Kimmeridge Clay Formation (Upper Jurassic) in the RGGE Project boreholes at Swanworth Quarry and Metherhills, south Dorset. *Proceedings of the Geologists' Association*, **111**, 265–280, https://doi.org/10.1016/S0016-7878(00)80019-X

Gallois, R.W. & Medd, A.W. 1979. Coccolith-rich marker bands in the English Kimmeridge Clay. *Geological Magazine*, **116**, 247–260, https://doi.org/10.1017/S0016756800043740

Goldberg, E.D. 1954. Marine geochemistry 1. Chemical scavengers of the sea. *The Journal of Geology*, **62**, 249–265, https://doi.org/10.1086/626161

Gradstein, F.M., Ogg, J.G., Schmitz, M. & Ogg, G. 2012. *The Geologic Time Scale 2012*. Elsevier, Boston.

Grygar, T.M., Mach, K. & Martinez, M. 2019. Checklist for the use of potassium concentrations in siliciclastic sediments as paleoenvironmental archives. *Sedimentary Geology*, **382**, 75–84, https://doi.org/10.1016/j.sedgeo.2019.01.010

Hakimi, M., Abdullah, W. & Shalaby, M. 2010. Source rock characterization and oil generating potential of the Jurassic Madbi Formation, onshore East Shabowah oilfields, Republic of Yemen. *Organic Geochemistry*, **41**, 513–521, https://doi.org/10.1016/j.orggeochem.2009.12.011

Hammer, Ø., Collignon, M. & Nakrem, H. A. 2012. Organic carbon isotope chemostratigraphy and cyclostratigraphy in the Volgian of Svalbard. *Norwegian Journal of Geology*, **92**, 103–112.

Hammes, U., Hamlin, S. & Ewing, T. 2011. Geologic analysis of the Upper Jurassic Haynesville Shale in east Texas and west Louisiana. *AAPG Bulletin*, **95**, 1643–1666, https://doi.org/10.1306/02141110128

Herbin, J. P. & Geyssant, J. R. 1993. Organic belts during Kimmeridgian/Tithonian in England (Yorkshire, Dorset) and France (Boulonnais) *Comptes Rendus de L'Academie des Sciences Seris II*, **317**, 1309–1316.

Herbin, J.P., Muller, C., Geyssant, J., Melieres, F. & Penn, I. 1991. *Heterogeneity of organic matter distribution in relation to a transgressive systems tract: Kimmeridge Clay (Jurassic), England*. AAPG Bulletin, 75, Dallas, TX.

Herbin, J.P., Müller, C., Geyssant, J.R., Mélières, F., Penn, I.E. & Group, Y. 1993. Variation of the distribution of organic matter within a transgressive system tract: Kimmeridge Clay (Jurassic), England. In: Katz, B.J. & Pratt, L.M. (eds) *Source Rocks in A Sequence Stratigraphic Framework*, AAPG Studies in Geology, **37**, 67–100, https://doi.org/10.1306/St37575C6

Herbin, J.P., Fernandez-Martinez, J.L. *et al.* 1995. Sequence stratigraphy of source rocks applied to the study of the Kim meridgian/Tithonian in the north-west European shelf (Dorset/UK, Yorkshire/UK and Boulonnais/France). *Marine and Petroleum Geology*, **12**, 177–194, https://doi.org/10.1016/0264-8172(95)92838-N

Hesselbo, S.P., Deconinck, J.-F., Huggett, J. & Morgans-Bell, H. 2009. Late Jurassic palaeoclimatic change from clay mineralogy and gamma-ray spectrometry of the Kimmeridge Clay, Dorset, UK. *Journal of the Geological Society, London*, **166**, 1123–1134, https://doi.org/10.1144/0016-76492009-070

Huang, Z., Williamson, M., Fowler, M. & McAlpine, K. 1994. Predicted and measured petrophysical and geochemical characteristics of the Egret Member oil source rock, Jeanne d'Arc Basin, offshore eastern Canada. *Marine and Petroleum Geology*, **11**, 294–306, https://doi.org/10.1016/0264-8172(94)90051-5

Huckriede, H. & Meischner, D. 1996. Origin and environment of manganese-rich sediments within black-shale basins. *Geochimica et Cosmochimica Acta*, **60**, 1399–1413, https://doi.org/10.1016/0016-7037(96)00008-7

Jenkyns, H.C. 2003. Evidence for rapid climate change in the Mesozoic–Palaeogene greenhouse world. *Philosophical Transactions of the Royal Society of London. Series A: Mathematical, Physical and Engineering Sciences*, **361**, 1885–1916, https://doi.org/10.1098/rsta.2003.1240

Jenkyns, H.C., Hesselbo, S.P., Jones, C.E., Gröcke, D.R. & Parkinson, D.N. 2002. Chemostratigraphy of the Jurassic System: applications, limitations and implications for palaeoceanography. *Journal of the Geological Society*, **159**, 351–378, https://doi.org/10.1144/0016-764901-130

Kemp, D.B., Fraser, W.T. & Izumi, K. 2018. Stratigraphic completeness and resolution in an ancient mudrock succession. *Sedimentology*, **65**, 1875–1890, https://doi.org/10.1111/sed.12450

Koevoets, M.J., Abay, T.B., Hammer, Ø. & Olaussen, S. 2016. High-resolution organic carbon -isotope stratigraphy of the Middle Jurassic -Lower Cretaceous Agardhfjellet Formation of central Spitsbergen, Svalbard. *Palaeogeography, Palaeoclimatology, Palaeoecology*, **449**, 266–274, https://doi.org/10.1016/j.palaeo.2016.02.029

Koevoets, M.J., Hammer, Ø., Olaussen, S., Senger, K. & Smelror, M., 2018. Integrating subsurface and outcrop data of the middle Jurassic to Lower Cretaceous Agardhfjellet formation in central Spitsbergen. *Norwegian Journal of Geology*, **98**, 1–34, https://dx.doi.org/10.17850/njg98-4-01

Lallier-Vergès, E., Bertrand, P., Huc, A.Y., Bückel, D. & Tremblay, P. 1993. Control of the preservation of organic matter by productivity and sulphate reduction in Kimmeridgian shales from Dorset (UK). *Marine and Petroleum Geology*, **10**, 600–605, https://doi.org/10.1016/0264-8172(93)90062-W

Lallier-Vergès, E., Hayes, J.M., Boussafir, M., Zaback, D.A., Tribovillard, N.P., Connan, J. & Bertrand, P. 1997. Productivity-induced sulphur enrichment of hydrocarbon-rich sediments from the Kimmeridge Clay Formation. *Chemical Geology*, **134**, 277–288, https://doi.org/10.1016/S0009-2541(96)00093-9

Lazar, O.R., Bohacs, K.M., Schieber, J., Macquaker, J.H. & Demko, T.M. 2015. *Mudstone Primer: Lithofacies Variations, Diagnostic Criteria, and Sedimentologic-stratigraphic Implications at Lamina to Bedset Scales*. SEPM (Society for Sedimentary Geology), Tulsa, OK.

Lees, J.A., Bown, P.R., Young, J.R. & Riding, J.B. 2004. Evidence for annual records of phytoplankton productivity in the Kimmeridge Clay Formation coccolith stone bands (Upper Jurassic, Dorset, UK). *Marine Micropaleontology*, **52**, 29–49, https://doi.org/10.1016/j.marmicro.2004.04.005

Macquaker, J. & Gawthorpe, R. 1993. Mudstone lithofacies in the Kimmeridge Clay Formation, Wessex Basin, southern England: implications for the origin and controls of the distribution of mudstones. *Journal of Sedimentary Research*, **63**.1129-1143, https://doi.org/10.1306/D4267CC1-2B26-11D7-8648000102C1865D

Macquaker, J.H.S., Keller, M.A. & Davies, S.J. 2010. Algal blooms and marine snow: mechanisms that enhance preservation of organic carbon in ancient fine-grained sediments. *Journal of Sedimentary Research*, **80**, 934–942, https://doi.org/10.2110/jsr.2010.085

Morgans-Bell, H., Coe, A. *et al.* 2001. Integrated stratigraphy of the Kimmeridge Clay Formation (Upper Jurassic) based on exposures and boreholes in south Dorset, UK. *Geological Magazine*, **138**, 511–539, https://doi.org/10.1017/S0016756801005738

Moshrif, M.A. 1984. Sequential Development of Hanifa Formation (upper Jurassic) Paleocnvironments and Paleogeography, Central Saudi Arabia. *Journal of Petroleum Geology*, **7**, 451–460, https://doi.org/10.1111/j.1747-5457.1984.tb00889.x

Negri, A., Ferretti, A. & Wagner, T. 2009. Organic-carbon-rich sediments through the Phanerozoic: processes, progress, and perspectives. *Palaeogeography Palaeoclimatology Palaeoecology, (Special Issue)*, **273**, 213–410, https://doi.org/10.1016/j.palaeo.2008.10.002

Neretin, L.N., Böttcher, M.E., Jørgensen, B.B., Volkov, I.I., Lüschen, H. & Hilgenfeldt, K. 2004. Pyritization processes and greigite formation in the advancing sulfidization front in the upper Pleistocene sediments of the Black Sea 1. *Geochimica et Cosmochimica Acta*, **68**, 2081–2093, https://doi.org/10.1016/S0016-7037(03)00450-2

Pancost, R., Van Dongen, B., Esser, A., Morgans-Bell, H., Jenkyns, H. & Sinninghe Damsté, J. 2005. Variation in Organic Matter Composition and Its

Impact on Organic-Carbon Preservation in the Kimmeridge Clay Formation (Upper Jurassic, Dorset, southern England). *In*: Harris, N.B. (ed.) *The deposition of organic-carbon-rich Sediments: Models, Mechanisms, and Consequences*. Special Publications of the Society for Sedimentary Geology (SEPM), **82**, Tulsa, OK, 261–278, http://dx.doi.org/10.2110/pec.05.82.0001

Pathak, D.B. 2007. Jurassic/Cretaceous boundary in the Spiti Himalaya, India. *Journal of the Palaeontological Society of India*, **52**, 51–57.

Pearce, C., Coe, A. & Cohen, A. 2010. Seawater redox variations during the deposition of the Kimmeridge Clay Formation, United Kingdom (Upper Jurassic): evidence from molybdenum isotopes and trace metal ratios. *Paleoceanography*, **25**, PA4213, https://doi.org/10.1029/2010PA001963

Pearson, S., Marshall, J. & Kemp, A. 2004. The Whitestone Band of the Kimmeridge Clay: an integrated high-resolution approach to understanding environmental change. *Journal of the Geological Society, London*, **161**, 675–683, https://doi.org/10.1144/0016-764903-089

Raiswell, R., Newton, R. & Wignall, P. 2001. An indicator of water-column anoxia: resolution of biofacies variations in the Kimmeridge Clay (Upper Jurassic, U.K.). *Journal of Sedimentary Research*, **71**, 286–294, https://doi.org/10.1306/070300710286

Ramanampisoa, L. & Disnar, J.R. 1994. Primary control of paleoproduction on organic matter preservation and accumulation in the Kimmeridge rocks of Yorkshire (UK). *Organic Geochemistry*, **21**, 1153–1167, https://doi.org/10.1016/0146-6380(94)90160-0

Riboulleau, A., Derenne, S., Sarret, G., Largeau, C., Baudin, F. & Connan, J. 2000. Pyrolytic and spectroscopic study of a sulphur-rich kerogen from the "Kashpir oil shales" (Upper Jurassic, Russian platform). *Organic Geochemistry*, **31**, 1641–1661. https://doi.org/10.1016/S0146-6380(00)00088-7

Rudnick, R.L. & Gao, S. 2003. Composition of the continental crust. *Treatise on Geochemistry*, **3**, 659.

Ruffell, A.H., Price, G.D., Mutterlose, J., Kessels, K., Baraboshkin, E. & Gröcke, D.R. 2002. Palaeoclimate indicators (clay minerals, calcareous nannofossils, stable isotopes) compared from two successions in the late Jurassic of the Volga Basin (SE Russia). *Geological Journal*, **37**, 17–33, https://doi.org/10.1002/gj.903

Sælen, G., Tyson, R.V., Telnæs, N. & Talbot, M.R. 2000. Contrasting watermass conditions during deposition of the Whitby Mudstone (Lower Jurassic) and Kimmeridge Clay (Upper Jurassic) formations, UK. *Palaeogeography, Palaeoclimatology, Palaeoecology*, **163**, 163–196, https://doi.org/10.1016/S0031-0182(00)00150-4

Sageman, B., Murphy, A., Werne, J., Ver Straeten, C., Hollander, D. & Lyons, T. 2003. A tale of shales: the relative roles of production, decomposition, and dilution in the accumulation of organic-rich strata, Middle–Upper Devonian, Appalachian basin. *Chemical Geology*, **195**, 229–273, https://doi.org/10.1016/S0009-2541(02)00397-2

Schieber, J. 2016. Mud re-distribution in epicontinental basins – exploring likely processes. *Marine and Petroleum Geology*, **71**, 119–133, https://doi.org/10.1016/j.marpetgeo.2015.12.014

Schnetger, B., Brumsack, H., Schale, H., Hinrichs, J. & Dittert, L. 2000. Geochemical characteristics of deep-sea sediments from the Arabian Sea: a high-resolution study. *Deep Sea Research Part II: Topical Studies in Oceanography*, **47**, 2735–2768, https://doi.org/10.1016/S0967-0645(00)00047-3

Sellwood, B.W. & Valdes, P.J. 2008. Jurassic climates. *Proceedings of the Geologists' Association*, **119**, 5–17, https://doi.org/10.1016/S0016-7878(59)80068-7

Shaw, A.B. 1964. *Time in Stratigraphy*, McGraw-Hill.

Taylor, S.R. & McLennan, S.M. 2001. Chemical composition and element distribution in the Earth's crust. *Encyclopedia of Physical Science and Technology*, 312.

Tribovillard, N.P., Desprairies, A., Lallier-Vergès, E., Bertrand, P., Moureau, N., Ramdani, A. & Ramanampisoa, L. 1994. Geochemical study of organic-matter rich cycles from the Kimmeridge Clay Formation of Yorkshire (UK): productivity versus anoxia. *Palaeogeography, Palaeoclimatology, Palaeoecology*, **108**, 165–181, https://doi.org/10.1016/0031-0182(94)90028-0

Tribovillard, N., Trentesaux, A., Ramdani, A., Baudinet, F. & Riboulleau, A. 2004. Controls on organic accumulation in late Jurassic shales of northwestern Europe as inferred from trace-metal geochemistry. *Bulletin de la Societe Geologique de France*, **175**, 491–506.

Tribovillard, N., Algeo, T.J., Lyons, T. & Riboulleau, A. 2006. Trace metals as paleoredox and paleoproductivity proxies: an update. *Chemical Geology*, **232**, 12–32, https://doi.org/10.1016/j.chemgeo.2006.02.012

Tribovillard, N., Algeo, T.J., Baudin, F. & Riboulleau, A. 2012. Analysis of marine environmental conditions based on molybdenum–uranium covariation—Applications to Mesozoic paleoceanography. *Chemical Geology*, **324**, 46–58, https://doi.org/10.1016/j.chemgeo.2011.09.009

Tribovillard, N., Hatem, E., Averbuch, O., Barbecot, F., Bout-Roumazeilles, V. & Trentesaux, A. 2015. Iron availability as a dominant control on the primary composition and diagenetic overprint of organic-matter-rich rocks. *Chemical Geology*, **401**, 67–82, https://doi.org/10.1016/j.chemgeo.2015.02.026

Tribovillard, N., Koched, H., Baudin, F., Adatte, T., Delattre, M., Abraham, R. & Ferry, J.N., 2019. Storm-induced concentration of sulfurized, marine-origin, organic matter as a possible mechanism in the formation of petroleum source-rock. *Marine and Petroleum Geology*, **109**, 808–818, https://doi.org/10.1016/j.marpetgeo.2019.07.003

Turner, B.W., Tréanton, J.A. & Slatt, R.M. 2016. The use of chemostratigraphy to refine ambiguous sequence stratigraphic correlations in marine mudrocks: an example from the Woodford Shale, Oklahoma, USA. *Journal of the Geological Society London,*, **173**, 854-868, https://doi.org/10.1144/jgs2015-125

Turner, H., Gradstein, F., Gale, A. & Watkins, D. 2017. The age of the Tojeira Formation (Late Jurassic, Early Kimmeridgian), of Montejunto, west-central Portugal. *Swiss Journal of Palaeontology*, **136**, 287–299, https://doi.org/10.1007/s13358-017-0137-6

Turner, H.E., Batenburg, S.J., Gale, A.S. & Gradstein, F.M. 2019. The Kimmeridge Clay Formation (Upper Jurassic–Lower Cretaceous) of the Norwegian Continental Shelf and Dorset, UK: a chemostratigraphic correlation. *Newsletters on Stratigraphy*, **52**, 1–32, https://doi.org/10.1127/nos/2018/0436

Tyson, R. 2004. Variation of marine total organic carbon through the type Kimmeridge Clay Formation (Late Jurassic), Dorset, UK. *Journal of the Geological Society, London*, **161**, 667–673, https://doi.org/10.1144/0016-764903-078

Van Kaam-Peters, H.M., Schouten, S., Köster, J. & Damstè, J.S.S. 1998. Controls on the molecular and carbon isotopic composition of organic matter deposited in a Kimmeridgian euxinic shelf sea: evidence for preservation of carbohydrates through sulfurisation. *Geochimica et Cosmochimica Acta*, **62**, 3259–3283, https://doi.org/10.1016/S0016-7037(98)00231-2

Waterhouse, H. 1999. Orbital forcing of palynofacies in the Jurassic of France and the United Kingdom. *Geology*, **27**, 511–514, https://doi.org/10.1130/0091-7613(1999)027<0511:OFOPIT>2.3.CO;2

Wedepohl, K. 1991. Chemical composition and fractionation of the continental crust. *Geologische Rundschau*, **80**, 207–223, https://doi.org/10.1007/BF01829361

Weedon, G.P., Coe, A.L. & Gallois, R.W. 2004. Cyclostratigraphy, orbital tuning and inferred productivity for the type Kimmeridge Clay (Late Jurassic), Southern England. *Journal of the Geological Society*, **161**, 655–666, https://doi.org/10.1144/0016-764903-073

Wignall, P.B. & Myers, K.J. 1988. Interpreting benthic oxygen levels in mudrocks: a new approach. *Geology*, **16**, 452–455, https://doi.org/10.1130/0091-7613(1988)016<0452:IBOLIM>2.3.CO;2

Wignall, P. & Newton, R. 1998. Pyrite framboid diameter as a measure of oxygen deficiency in ancient mudrocks. *American Journal of Science*, **298**, 537–552, https://doi.org/10.2475/ajs.298.7.537

Wignall, P.B. & Ruffell, A.H. 1990. The influence of a sudden climatic change on marine deposition in the Kimmeridgian of northwest Europe. *Journal of the Geological Society*, **147**, 365–371, https://doi.org/10.1144/gsjgs.147.2.0365

Williams, C.J., Hesselbo, S.P., Jenkyns, H.C. & Morgans-Bell, H.S. 2001. Quartz silt in mudrocks as a key to sequence stratigraphy (Kimmeridge Clay Formation, Late Jurassic, Wessex Basin, UK). *Terra Nova*, **13**, 449–455, https://doi.org/10.1046/j.1365-3121.2001.00378.x

Zuo, F., Heimhofer, U., Huck, S., Bodin, S., Erbacher, J. & Bai, H. 2018. Coupled δ13C and 87Sr/86Sr chemostratigraphy of Kimmeridgian shoal-water deposits: a new composite record from the Lower Saxony Basin, Germany. *Sedimentary Geology*, **376**, 18–31, https://doi.org/10.1016/j.sedgeo.2018.07.012

Zuo, F., Heimhofer, U., Huck, S., Adatte, T., Erbacher, J. & Bodin, S. 2019. Climatic fluctuations and seasonality during the Kimmeridgian (Late Jurassic): stable isotope and clay mineralogical data from the Lower Saxony Basin, Northern Germany. *Palaeogeography, Palaeoclimatology, Palaeoecology*, **517**, 1–15, https://doi.org/10.1016/j.palaeo.2018.12.018